

# PING-Mapper: open-source software for automated benthic imaging and mapping using recreation-grade sonar

This is a Preprint and has not been peer reviewed.

## Authors:

Cameron S. Bodine, *csb67@nau.edu*

School of Informatics, Computing, and Cyber Systems, Northern Arizona University, Flagstaff, Arizona, USA.

Daniel Buscombe

School of Informatics, Computing, and Cyber Systems, Northern Arizona University, Flagstaff, Arizona, USA.

School of Earth and Sustainability, Northern Arizona University, Flagstaff, Arizona, USA.

Rebecca J. Best

School of Earth and Sustainability, Northern Arizona University, Flagstaff, Arizona, USA.

Jennylyn A. Rednert

Arizona Natural Heritage Program, Arizona Game and Fish Department, Phoenix, Arizona, USA..

Adam J. Kaeser

U.S. Fish and Wildlife Service, Panama City Fish and Wildlife Conservation Office, Panama City, Florida, USA.

## Key Points:

- We developed an open-source software for exporting benthic datasets and georeferenced imagery from Humminbird side scan sonar systems.
- Software provides automated and reproducible approach to processing sonar data with minimal interaction from the user.
- Three case studies are presented to highlight use cases of processed benthic datasets.

June 13, 2022

Associated software, PING-Mapper: <https://github.com/CameronBodine/PINGMapper>

# PING-Mapper: open-source software for automated benthic imaging and mapping using recreation-grade sonar

C. S. Bodine<sup>1</sup>, D. Buscombe<sup>1,2</sup>, R. J. Best<sup>2</sup>, J. A. Redner<sup>3</sup>, and A. J. Kaeser<sup>4</sup>

<sup>1</sup>School of Informatics, Computing, and Cyber Systems, Northern Arizona University, Flagstaff, Arizona, USA.

<sup>2</sup>School of Earth and Sustainability, Northern Arizona University, Flagstaff, Arizona, USA.

<sup>3</sup>Arizona Natural Heritage Program, Arizona Game and Fish Department, Phoenix, Arizona, USA.

<sup>4</sup>U.S. Fish and Wildlife Service, Panama City Fish and Wildlife Conservation Office, Panama City, Florida, USA.

June 13, 2022

## Abstract

*The characterization of benthic habitats is essential for aquatic ecosystem science and management, but is frequently limited by waterbody visibility and depth. Recreation-grade side scan sonar systems are increasingly used to aid scientific inquiries in shallow water due to their relative low-cost, ease of operation, low-weight, and ease of mounting on a variety of vessels. However, existing procedures and software for post-processing these data are either limited, closed source, or fail on data from new sonar models; limiting development of reproducible workflows. Here we present PING-Mapper, an open source and freely available side scan sonar post-processing toolset for processing and mapping sonar recordings from popular Humminbird instruments. The modular software automatically: 1) decodes sonar recordings from any Humminbird system; 2) exports ping attributes from every sonar channel; 3) uses sonar sensor depth for water column removal; and 4) exports sonogram tiles and georectified mosaics. Sonar channels are processed in parallel for quick decoding and metadata extraction. Workflows for major processing workflows including georectification and image export scale with computing resources. The software has been extensively tested using data from several river distributaries of varying character and distribution of depths, but could also be used in estuarine and lacustrine environments. Usage of PING-Mapper is illustrated in three case studies focused on mapping large woody debris, bathymetric mapping, and visual interpretation and mapping of substrates for select reaches of the Pearl and Pascagoula river systems in Mississippi.*

**Keywords**– Acoustic remote sensing, Sidescan sonar, Benthic habitat

## Plain Language Summary

Side scan sonar instruments provide a way to survey and visualize the bottom of rivers, lakes, or oceans. Since the early 2000s, companies catering predominantly to anglers have manufactured recreation-grade side scan sonar systems to aid fishermen in locating fish and identifying potential hazards. Scientists seeking to understand and manage aquatic habitats soon found use in these systems to create grayscale images of water bottoms because they are inexpensive, are easy to operate, and require minimal mounting equipment on the boat. Software has been created by companies to process these data, but the underlying processing workflow and computer code are not publicly available, which makes it difficult to reproduce and compare results among multiple scientists and studies. Other publicly available approaches and software are either outdated, not maintained, or not free. That is why we made PING-Mapper. This software is built using a programming language called Python, an increasingly popular language used by many

35 scientists. All the code of PING-Mapper is made freely available. We designed the soft-  
36 ware to work on any computer with minimal hardware specifications, to export the de-  
37 sired datasets as quickly as possible. We demonstrate the use of the exported datasets  
38 with three case studies focused on common scientific usages, locating and mapping tar-  
39 gets (specifically large trees and branches), creating depth maps, and visually discern-  
40 ing the distributions of common substrates such as sand and cobble.

## 41 1 Introduction

42 Our understanding of the Earth’s surface and atmosphere has benefited from large  
43 investments in air and space-borne observation systems, such as NASA’s Earth Obser-  
44 vation System (EOS) (Murphy, 2021), providing unparalleled ability to model the cli-  
45 mate (Yang et al., 2013), track landcover changes (Weiers et al., 2004; Bock et al., 2005),  
46 or map species-specific habitat availability (Kerr & Ostrovsky, 2003). In comparison, the  
47 spatial and temporal extent of our knowledge of aquatic environments, particularly shal-  
48 low freshwater habitats, remains limited. This leaves scientists and managers with less  
49 information to address threats to species that depend on freshwater systems (Barnosky  
50 et al., 2011; Tickner et al., 2020). Shallow waterbodies are ubiquitous; 85% of the world’s  
51 3.5M rivers have an average depth of 1m (Andreadis et al., 2013), and the average depth  
52 of the world’s 27M lakes is 41.8m, with 99% of lakes less than 10m in depth (Cael et al.,  
53 2017). Shallow water, particularly small waterbodies (Biggs et al., 2017), are dispro-  
54 portionately important for aquatic biodiversity including macrophytes (Fu et al., 2014), bac-  
55 teria, diatoms and chironomids (Zhao et al., 2019); macrobenthos (Musale & Desai, 2010);  
56 plankton (Longhurst, 2007); pelagic fish (Smith & Brown, 2002); and assemblages of ma-  
57 rine meiofauna, macrofauna, and megafauna (Danovaro et al., 2010).

58 Techniques available for mapping in-stream habitat depend on the species of in-  
59 terest, type of system, parameters of interest, and spatial scale (Myrsvold & Dervo, 2020),  
60 however traditional techniques for collecting these parameters are limited in space and  
61 time. Side scan sonar (SSS) is an effective technology for efficiently collecting large swaths  
62 of benthic imagery (Chesterman et al., 1958; Klein & Edgerton, 1968; Singh et al., 2000;  
63 Brown et al., 2011). Sonar images are geographically rectified (i.e., georectified), con-  
64 verting time and slant-range distance data into a regular Cartesian grid positioned ac-  
65 curately in space using geographic positioning system (GPS) coordinates. Survey-grade  
66 systems popular for imaging marine ecosystems are relatively expensive and require sub-  
67 stantial technical expertise. It is also more difficult and dangerous to operate hydrographic  
68 survey vessels in shallow water. Recreation, or consumer-grade sonar systems (e.g., Hum-  
69 minbird, Lowrance, and Garmin) offer an alternative and are increasingly popular for  
70 scientific research (Kaeser & Litts, 2010; Schmidt et al., 2020; Scholl et al., 2021). These  
71 systems are comparatively low-cost, portable, and easy to operate and deploy; require  
72 minimal power and experience; and can be launched from small watercraft. However,  
73 extracting and processing data from these systems remains a major challenge. Leverag-  
74 ing the transformative potential of these systems for scientific research thus requires free  
75 and open-source software implementations of scientifically defensible processing work-  
76 flows that have been tested on a variety of data.

77 The first method to extract data from Humminbird Side Imaging systems to map  
78 shallow water habitat features was a sonar screen snapshot approach (Kaeser & Litts,  
79 2008, 2010). In this method, concurrent overlapping snapshots are captured at regular  
80 intervals via live feed imagery on the control head screen. Snapshots can be inadvertently  
81 missed, leaving gaps in resulting sonar mosaics. Snapshot image resolution is determined  
82 by the control head’s screen size, necessitating larger and more expensive systems. Af-  
83 ter data collection, tools developed by the authors require time-consuming manual post-  
84 processing steps to generate georectified mosaics, limiting batch processing options. The  
85 tools are written in Visual Basic for Applications (VBA) and run in potentially cost-prohibitive

86 ESRI ArcGIS software; however, current ArcGIS versions no longer support VBA, ef-  
87 fectively rendering this approach obsolete.

88 Many of the limitations of the snapshot approach can be overcome by recording  
89 sonar intensity and metadata directly to file, but format and structure are not provided  
90 by the manufacturer. Currently, options for processing these files are limited. Decod-  
91 ing recordings from early Humminbird models was first demonstrated with PyHum (Buscombe  
92 et al., 2016; Buscombe, 2017); an open-source Python toolbox for decoding sonar record-  
93 ings, exporting ping metadata (e.g., vessel position, heading, and speed), applying sonar  
94 intensity corrections, classifying bed textures, and exporting georectified imagery. The  
95 software is limited in application because it only works for older Humminbird models,  
96 is difficult to install due to underlying dependencies, and has poor computational effi-  
97 ciency. Alternatives to this toolbox have additional limitations. For example, HumViewer  
98 (Johansen, 2013) permits users to view the recording but offers limited export function-  
99 ality. HumConverter (Parnum et al., 2017) is a free software for decoding sonar record-  
100 ings but requires MATLAB (> 1,000 USD) to work with file exports. Low-cost (< 500  
101 USD) commercial software such as SonarTRX (Leraand Engineering Inc., 2022) and Reef-  
102 Master (ReefMaster Software Ltd., 2021) offer interfaces and tools for viewing, correct-  
103 ing, and exporting sonar data. However, source-code for these programs are not housed  
104 on public-repositories, limiting opportunities for collaboration, scientific applications re-  
105 quiring reproducibility, and modifications or extensions to functionality.

106 This article describes PING-Mapper, a new modular processing engine written in  
107 Python 3 that is open-source and free to use. It is similar in scope to PyHum, but works  
108 with data from all Humminbird models, is easier to install and maintain, and is more  
109 computationally efficient. We have also significantly improved the algorithms for depth  
110 detection, and image rectification, and have tested on a larger variety of environmental  
111 conditions. The software provides many advantages to the software and methodologies  
112 referenced here including: 1) decoding any Humminbird sonar recording, regardless of  
113 model (at the time of writing, there are 14 Humminbird side imaging models available);  
114 2) batch processing of sonar recordings; 3) export of ping metadata to comma separated  
115 value or CSV format files; 4) export of non-rectified imagery; 5) export of georectified  
116 imagery; and is 6) publicly hosted in a repository, ensuring workflow transparency, and  
117 inviting contributions from the community.

## 118 2 Implementation

119 The following sections describe PING-Mapper’s processing workflow (Figure 1) for  
120 decoding and exporting benthic datasets from Humminbird SSS systems.

### 121 2.1 Decode Humminbird Files

122 Sonar recording files from a Humminbird sonar instrument are written in a prop-  
123 rietary format of ASCII-encoded hexadecimal values. Each sonar scan creates a single  
124 DAT file. The DAT file stores metadata when a recording is initialized, including the  
125 selected water type (of which there are three; fresh, shallow saltwater, deep saltwater),  
126 the Unix time (epoch) in seconds, Easting and Northing in World Geodetic System 1984  
127 (WGS 84) World Mercator coordinate reference system, name of the recording, number  
128 of pings, initial range setting (i.e., number of ping returns), and length of the record-  
129 ing in milliseconds.

130 Along with the DAT file, each active sonar channel, or beam, has an associated SON  
131 and IDX file. The SON file stores the pings while the IDX file stores the byte index (the  
132 location in the file of the start of each ping) and time elapsed of each ping in the SON  
133 file. A ping has two components: 1) ping attributes (termed here as ping header, or sim-

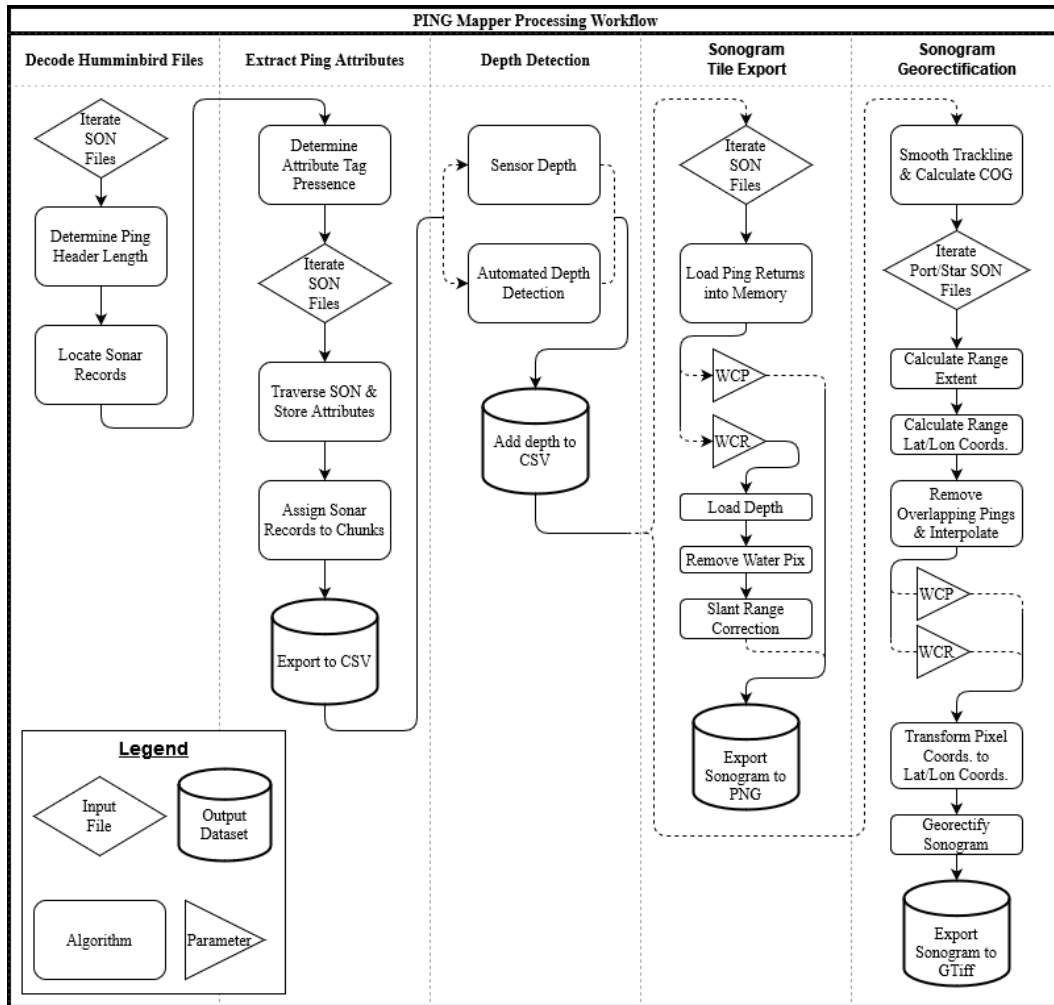


**Figure 1.** Overview of PING-Mapper processing workflow as described in Section 2. Acronyms are defined as: SON (Humminbird sonar file); CSV (comma-separated values file); WCP (water column present); WCR (water column removed); PNG (portable network graphics); COG (course over ground, i.e., heading); Lat (latitude); Lon (longitude); and GTiff (geospatial tag image file format).

ply header); and 2) ping returns, or acoustic backscatter intensity values, stored in 8-bit [0-255] encoding (Buscombe, 2017).

The number of bytes in a ping vary in two ways. First, the length of the header is dependent on the Humminbird model, with each model storing a varying number of ping attributes (see Supporting Information Table 1). Regardless of the header contents, each starts and ends with the same values, allowing PING-Mapper to automatically determine header length. Second, the ping length (in milliseconds) varies with the number of returns following the header, determined by the range setting at the time of the survey, which in turn dictates the sonar pulse length (Buscombe, 2017). The last attribute in the header indicates the number of returns that follow. The next ping immediately follows the last return of the previous ping, and so on. The IDX file allows quick navigation to the beginning of each sonar record, but these files can become corrupt due to, for example, power failure during the survey. If the IDX file is corrupt or missing, PING-Mapper locates pings based on the header length and number of returns.

## 2.2 Extract Ping Attributes

For each ping in a SON file, the header stores a series of attributes relating to that ping's returns. Each attribute is tagged with a unique identifier, or name, followed by the attribute's value. All sonar models use consistent naming of a given attribute, but may have additional unused attribute slots. Once pings are located, PING-Mapper decodes each header and exports the attributes to a CSV for each sonar beam. Attributes with valid data contain positional information, time elapsed, depth at nadir, heading, and speed. A list of all attributes and their location based on sonar model is provided in Table 1. These data are used in subsequent georectification procedures, which convert the raw data into a regular spatial grid that can be viewed as a map (see section 2.5).

## 2.3 Depth Detection

Water depth is a fundamental variable governing river hydraulics, morphologies, sediments, and habitats and is also used to make the necessary geometric corrections to the sonar imagery to recreate continuous planform imagery of the bottom (see sections 2.4-2.5). SSS systems are equipped with down-facing sonar beam(s) that imprecisely estimate the depth at nadir for each sonar record. These data are stored in the SON files for each ping. The estimates are often error-prone due to various mechanical and environmental factors (Yan et al., 2021). Therefore, options to smooth noisy estimates and uniformly adjust the depth to account for sonar transducer offset are provided.

## 2.4 Sonogram Tile Export

Once ping attributes have been extracted, non-rectified sonar imagery of ping returns, or sonograms, are optionally exported to tiles. PING-Mapper loads ping returns into memory in batches based on chunk size (see Section 2.6). Sonograms can be exported with the water column present (WCP) or water column removed (WCR). WCP images show the water column at nadir, making them suitable for applications of locating and counting fish (Flowers & Hightower, 2013) as well as measuring height of submerged vegetation (Sánchez-Carnero et al., 2012). WCP images require no additional post-processing and can be directly exported to standard image formats. Alternatively, WCR images are most suitable for accurate spatial positioning of the bed as presence of the water column introduces geometric distortions which affect of the bed pixels in the near-field (Cobra et al., 1992), necessitating additional post-processing to generate these sonograms.

A two-step geometric correction to the sonogram is required to remove the water column pixels then relocate the bed pixels horizontally across the track, known as slant

182 range correction (Cobra et al., 1992). The sonar system cannot measure depth across  
 183 track, preventing precise calculation of across track distance, or range, to each pixel. There-  
 184 fore, a naïve assumption that the bed is flat across the track allows the range to be ap-  
 185 proximated using the slant range and depth at nadir. This flat-bed assumption applies  
 186 only to the useful portion of riverbed scanned, which is approximately 10-20 times the  
 187 water depth as a rule-of-thumb. The flat-bed assumption is calculated piecewise across  
 188 the width of the waterbody and bed pixels are redistributed across the track. Gaps in  
 189 the data are then filled using a one-dimensional piecewise linear interpolation method.  
 190 Non-rectified SRC sonogram tiles can then be exported to standard image formats.

## 191 2.5 Sonogram Georectification

192 Recreation-grade sonar systems often have an autonomous internal GPS receiver  
 193 in the sonar control head. Ports are available to add an external GPS that might have  
 194 better positional accuracy. Each sonar record has a single geographic coordinate and the  
 195 heading from the GPS. These data are used to warp the sonogram to the vessel track  
 196 and geographically locate each pixel, termed here georectification.

197 In a typical side scan survey, the vessel is constantly moving to image the bed. How-  
 198 ever, the GPS refresh rate is typically slower than the ping rate, resulting in multiple  
 199 sonar records sharing identical coordinates despite the constant movement of the ves-  
 200 sel. PING-Mapper performs several corrections to recalculate the coordinates for each  
 201 sonar record along the track. First, ping coordinates are filtered to ensure unique coor-  
 202 dinate pairs. Next, coordinates are filtered to decrease point density and speed the next  
 203 step of fitting a third-degree piecewise affine spline to the filtered coordinates. The spline  
 204 is parameterized using the sonar record’s unique id and the time elapsed. Finally, new  
 205 coordinates are then predicted for each sonar record using the spline, resulting in sonar  
 206 records with unique coordinate pairs along the smoothed vessel course spaced assum-  
 207 ing a constant speed. These steps further improve rectification of sonograms along sin-  
 208 uous river reaches.

## 209 2.6 Processing Large Recordings

210 The duration of a sonar survey and the range setting dictate the size of the sonar  
 211 recording file, which can become prohibitively large for a typical computer to process.  
 212 Therefore, PING-Mapper was designed to process sonar recordings in chunks. The chunk  
 213 size sets the number of ping returns that will be read into memory for each sonar beam.  
 214 A value of 500 is found to be appropriate in most scans but can be altered by users based  
 215 on available computing resources. This any modern computer to process sonar record-  
 216 ings of any size.

217 Another advantage to processing sonar recordings in chunks is that multiple chunks  
 218 can be processed concurrently. PING-Mapper supports multi-threaded processing to ex-  
 219 tract ping attributes, export non-rectified imagery, and sonogram georectification and  
 220 export, resulting in decreasing overall processing time. Tests were conducted on a 01h:00m:06s  
 221 sonar recording to determine speed of processing and data export. PING-Mapper is able  
 222 to process and export all possible data products in 00h:41m:14s on a typical computer.  
 223 Assuming a typical day in the field can result in upwards of 8h of sonar recordings, PING-  
 224 Mapper could be set to process the data over night with datasets ready for analysis the  
 225 next morning. Additional information is provided in Supplement Information Section  
 226 Computational Performance and Table 2.

## 227 3 Case Studies

228 The following three case studies illustrate some analyses that can be undertaken  
 229 with outputs from PING-Mapper. First, WCP sonar mosaics are used to locate and map

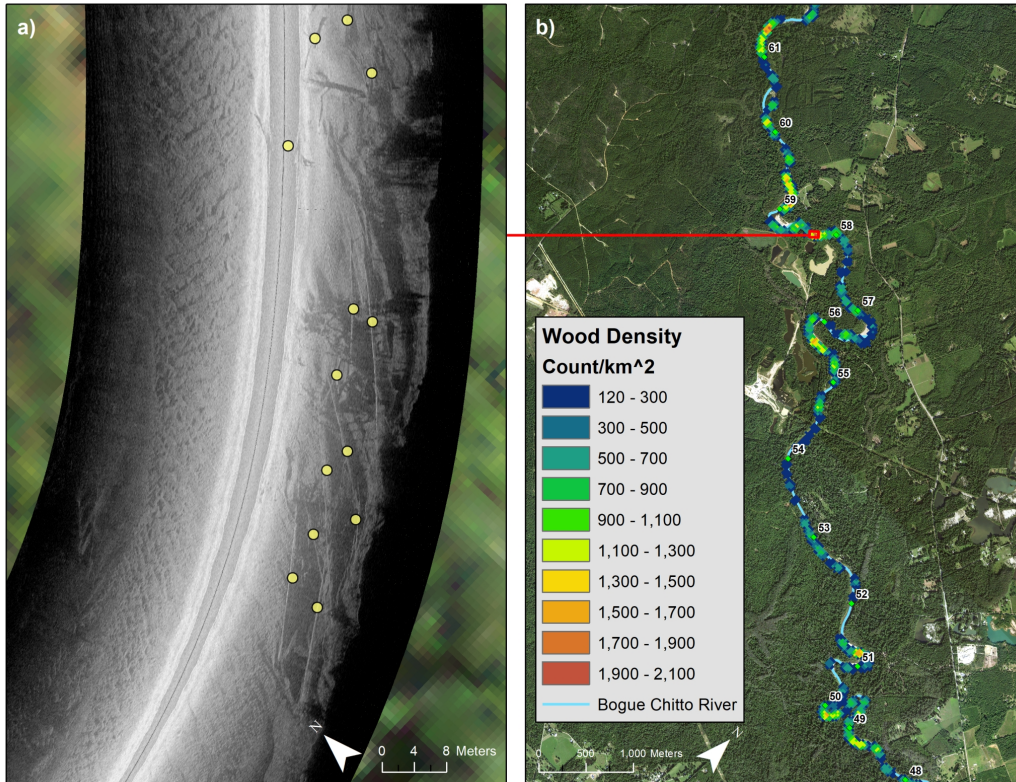


**Figure 2.** Example of locating and mapping large woody debris in the Bogue Chitto River in Mississippi. Panel (a) shows a georectified sonogram with water column present, with yellow points indicating location of large woody debris. Panel (b) shows wood density count per square kilometer.

230 large woody debris distribution in the Bogue Chitto River, MS. Second, sonar depth es-  
 231 timates from two survey transects on the Pearl River, MS allow creation longitudinal depth  
 232 profiles and basic bathymetric surfaces. Finally, WCR sonar mosaics are visually inter-  
 233 preted to identify and delineate substrates on the Leaf River, MS. All sonar data were  
 234 collected with a Humminbird Solix Chirp Mega SI+ sonar instrument operating at a nom-  
 235 inal central frequency of 1.2 MHz with unknown frequency bandwidth; however, simil-  
 236 ar results are expected from any modern Humminbird model.

### 237 3.1 Mapping Large Woody Debris

238 Large woody debris present in aquatic environments serve important ecological func-  
 239 tions for various species (Dolloff & Warren, 2003). Surveying rivers with SSS has proven  
 240 successful in locating large-woody debris (Holcomb et al., 2020; Kaeser & Litts, 2008).  
 241 SSS data were collected on the Bogue Chitto River, MS approximately 54 to 63 river kilo-  
 242 meters (RKM) upstream of the confluence with the Pearl River on March 2, 2021. The  
 243 sonar data were post-processed using PING-Mapper and georectified sonograms with the  
 244 water column present were exported. Large woody debris were visually identified in a  
 245 GIS by their distinguishing characteristic of long, linear edges and the shadows that they  
 246 cast. Points were then placed on identified wood throughout the survey reach (Figure  
 247 2a). Finally, mapping the density of these points illustrates variation in wood presence  
 248 across river reaches (Figure 2b).



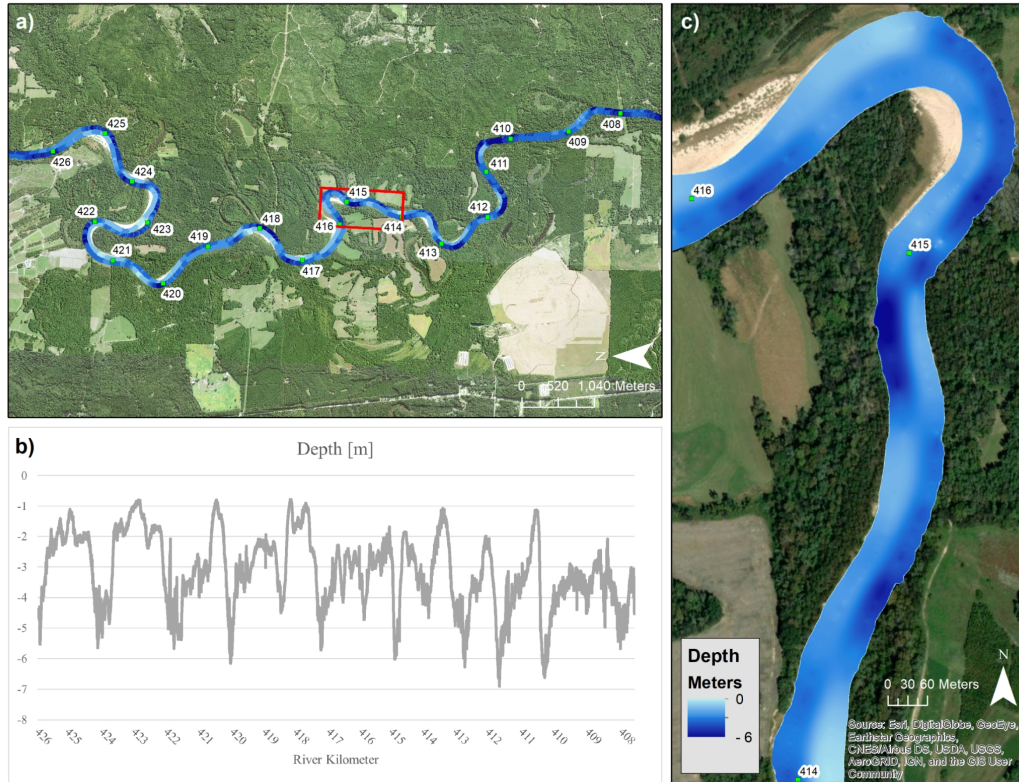


**Figure 3.** Example of mapping depth with SSS. Panel (a) shows sonar depths from two adjacent survey transects across 18 river kilometers on the Pearl River in Mississippi, surveyed upstream (RKM 426) to downstream (RKM 408). Panel (b) shows depth readings from the transect on the right side of the channel. Panel (c) shows an interpolated surface derived from the two transects and constrained by manually digitized banklines. To digitize the banklines, WCR georectified mosaics were exported and brought into a GIS where they were visually interpreted to determine the location of the bank, and a polyline was digitized along the bank.

249

### 3.2 Mapping Bathymetry

250

251

252

253

254

255

256

257

258

259

Two SSS survey transects from two vessels spaced to reduce interference were conducted on the Pearl River, MS on March 4, 2021, from RKM 426 to 408. One vessel surveyed the left side of the channel and the other right, moving upstream to downstream. Sonar depth estimates from down-facing beams are shown for two transects (Figure 3a) and a longitudinal profile for the river-right transect (Figure 3b) shows that our software is able to position and map the sonar data to capture the complex bathymetry in the sequence of riffles and pools. The sonogram mosaics and satellite imagery were used to delineate channel bank lines in a geographic information system (GIS). The bank lines constrained an inverse distance weighting (IDW) interpolation of the two transects to generate a bathymetric surface (Figure 3c).

260

### 3.3 Mapping Substrate

261

262

263

Scanning a waterbody with SSS results in imagery with tones and textures that can be associated with different types of substrate (Kaesler & Litts, 2010). Once georectified, the sonograms are brought into a GIS for visual interpretation and manual delin-

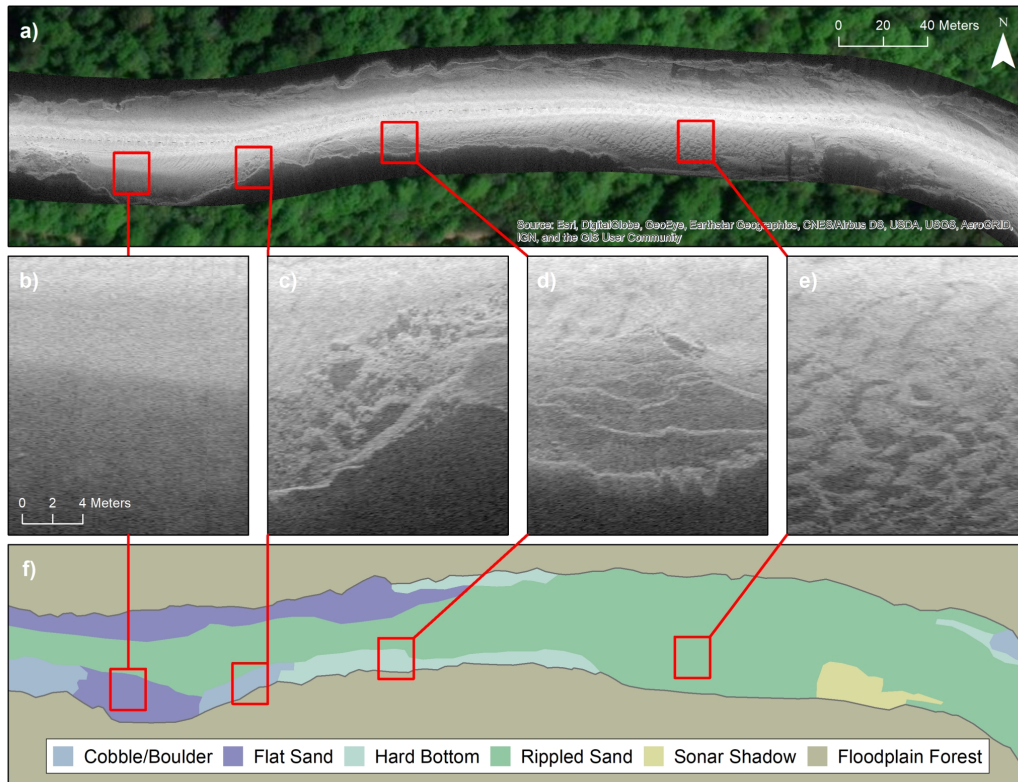


**Figure 4.** Example of delineating and classifying substrate on the Leaf River, MS. Panel (a) shows georectified sonograms with the water column removed. Detail views of the sonograms show (b) flat sand; (c) cobble/boulder; (d) hard bottom; and (e) rippled sand. Panel (f) shows a map of the substrate boundaries visually identified and manually delineated in a GIS.

264 eation of polygons, resulting in maps showing coverage and distribution of substrates at  
 265 large spatial extents. The Leaf River, MS, was scanned 138 RKM upstream of the Pascagoula  
 266 River confluence on May 6, 2021. The sonar recordings were processed with PING-Mapper  
 267 and georectified sonograms with the water column removed were exported (4a). Differ-  
 268 ent substrate types were visually identified and polygons were manually digitized in a  
 269 GIS to delineate substrate boundaries. Smooth, homogeneous textures are associated  
 270 with flat sand bedforms (4b); blocky textures with shadows are associated with boulder  
 271 and cobble (4c); sharp edges indicating terracing are associated with hard bottom  
 272 (4d); and wavy, chevron textures with shadows are associated with rippled sand (4e).  
 273 Portions of the sonogram with the same substrate characteristics were delineated with  
 274 a polygon, resulting in a map of substrate distribution (4f).

## 275 4 Discussion

276 PING-Mapper is a new Python toolbox for decoding and exporting benthic datasets  
 277 from Humminbird SSS instruments. It builds and improves upon previous algorithms  
 278 (Buscombe, 2017) for depth detection and georectification, and speeds processing and  
 279 export. The software is designed to 1) decode sonar recordings from any Humminbird  
 280 system; 2) export ping attributes from every sonar channel; 3) use sonar sensor depth  
 281 for water column removal; and 4) exports sonogram tiles and georectified mosaics. The  
 282 software are hosted in a public repository to ensure equitable access.

283 Aquatic scientists are increasingly using SSS to inform a range of research efforts.  
 284 This includes mapping essential habitats (Kaeser & Litts, 2008; Cheek et al., 2016; Walker  
 285 & Alford, 2016; Holcomb et al., 2020), informing invasive species competition for discrete  
 286 habitat patches (Gocłowski et al., 2013; Prechtel et al., 2018), enhancing habitat mod-  
 287 eling for aquatic species (Smit & Kaeser, 2016; Kaeser et al., 2019), and mapping aquatic  
 288 vegetation (Gumusay et al., 2019). Studies like these depend on the ability to easily con-  
 289 vert output from recreation-grade sonar systems into reproducible datasets with min-  
 290 imal expertise in data processing. PING-Mapper provides a suite of algorithms to fa-  
 291 cilitate this conversion. More importantly, these tools generate large datasets quickly which  
 292 allow scientific studies to be conducted at increasing spatial and temporal scales rele-  
 293 vant to numerous disciplines in ecological, environmental, and physical sciences concerned  
 294 with the form and character of benthic environments and the life they support.

295 The creation of a recreation-grade sonar processing pipelines allows opportunities  
 296 for future research, analysis, and applications of datasets generated by PING-Mapper.  
 297 For example, a primary use of side scan sonar image mosaics is to locate and map sub-  
 298 strate distributions throughout aquatic systems. Visual identification and manual dig-  
 299 itization is common practice (Kaeser et al., 2013) but automated machine learning ap-  
 300 proaches such as Buscombe and Goldstein (2022) show promise. Future work will focus  
 301 on developing and integrating automated substrate segmentation and classification work-  
 302 flows to inform landscape-level aquatic studies. Reliable depth measurements are nec-  
 303 essary to ensure accurate spatial positioning and coverage of automated substrate maps  
 304 generated from sonogram mosaics, therefore automated depth detection routines such  
 305 as Zheng et al. (2021) will be incorporated in the future. Potential improvements for the  
 306 marine environment include implementing attitude adjustment (i.e., pitch, yaw and roll)  
 307 and incorporating salinity to better locate the bed (Blondel, 2009).

308 The goal of this software is to address the growing and evolving data processing  
 309 needs of the aquatic research community by including recreation-grade sonar datasets  
 310 in their research. Particular emphasis has been placed on making PING-Mapper an open  
 311 source tool for benthic applications and research. The code is designed to be modular  
 312 and object oriented to facilitate contributions, modifications, and new applications from  
 313 the community. This software is the first of its kind in that it allows any engaged cit-  
 314 izen or researcher working in any aquatic waterbody to image their system with zero soft-  
 315 ware costs and full reproducibility.

## 316 Data Availability Statement

317 The code for PING-Mapper and test sonar recordings are available on Zenodo and  
 318 GitHub via Bodine and Buscombe (2022).

## 319 Acknowledgments

320 This study was made possible by a partnership between the U.S. Fish and Wildlife  
 321 Service and Northern Arizona University. Funding for this work was provided by the Open  
 322 Ocean Restoration Area Trustee Implementation Group of the Deepwater Horizon Trustee  
 323 Council as part of their Final Restoration Plan 1 for birds and sturgeon. The findings  
 324 and conclusions in this article are those of the authors and do not necessarily represent  
 325 the views of the U.S. Fish and Wildlife Service. Thanks to Channing St. Aubin (USFWS),  
 326 Mike Andres (USM), Eric Haffey (USM), Kasea Price (USM), and Katherine Wright (USM)  
 327 for data collection and planning, and to Daniel Haught (USGS) for testing.

## 328 Supporting Information

## 329 Computational Performance

330 The software is designed to speed processing and dataset export through multi-threaded  
331 processing. Export of plots, tiles and rectified sonograms account for the largest propor-  
332 tion of the total processing time, therefore running these algorithms in parallel result in  
333 significant decrease in total processing time. Algorithms which were parallelized include  
334 decoding and export of SON ping metadata, export of bedpick plots, export of sonogram  
335 tiles, and export of rectified sonogram GeoTiffs. Portions of the software that run se-  
336 quentially (e.g., non-parallelized) include decode and export of DAT metadata, deter-  
337 mining SON file structure, depth processing, trackline smoothing, and mosaic rectified  
338 sonograms.

339 The computational performance of PING-Mapper was tested with a sonar record-  
340 ing from a Humminbird Helix with Mega imaging. Sonar recording includes high-frequency  
341 down image (200 kHz), very high-frequency down image (1.2 MHz), and two very high-  
342 frequency side scan images (1.2 MHz). Total duration of the recording is 01:00:06 (hh:mm:ss).  
343 Total ping count is 279,916. Range setting is 1,398 returns per ping, or 26.6m. Chunk  
344 size is set to 512 pings, resulting in the following exports: 547 WCP sonograms; 274 WCR  
345 sonograms; 137 bedpick plots; 274 WCP rectified GeoTiffs; 274 WCR rectified GeoTiffs;  
346 and mosaics for WCP and WCR.

347 Tests were run on a Windows 10 laptop with Intel i7-8650U 1.90 GHz CPU, 16 GB  
348 of memory, and 500 GB solid state hard drive. Each test was run with an increasing num-  
349 ber of processing threads ( $t$ ), including  $t = 1, 2, 4, 6,$  and  $8$  threads. All other param-  
350 eters remained the same. Processing time, in seconds, are shown for the main compo-  
351 nents of the software in Table 2. Total processing time is reported in seconds as well as  
352 hours, minutes, and seconds (hh:mm:ss) for reference. Sequential algorithm processing  
353 time remained approximately constant with varying number of process threads. The al-  
354 gorithm for decoding SON scales with number of threads until the number of threads  
355 is equal to the number of beams, then remains roughly constant for  $t > 4$ . The algo-  
356 rithms to export bedpick plots, sonogram tiles, and rectify sonograms had decreasing pro-  
357 cessing time with increasing  $t$ .

**Table 1.** Humminbird SON file structure for specified sonar models: 9xx series, 11xx series, Helix, Onyx, and Solix. Other models presumably follow a similar pattern. The Name and Description indicate the type of data available for each ping in a Humminbird sonar recording. The Hex Tag is the 8-bit hexadecimal value preceding the data value. For each of the Humminbird models, the offset from the beginning of the recording is given for the respective data type. This pattern repeats for each ping for the duration of the sonar recording.

Name	Description	Hex Tag	Data Offset (by model)		
			9xx	11xx; Helix; Onyx	Solix
Ping #1	Beginning of ping #1	C0	+0	+0	+0
Header Start	Beginning of ping header	21	+3	+3	+3
Record Number	Unique ping ID	80	+5	+5	+5
Time Elapsed	Time elapsed (msec)	81	+10	+10	+10
UTM X	EPSG 3395 easting coord.	82	+15	+15	+15
UTM Y	EPSG 3395 northing coord.	83	+20	+20	+20
Heading Quality	Quality flag <sup>1</sup>	84	+25	+25	+25
Heading	Heading (1/10 deg)	-	+27	+27	+27
Speed Quality	Quality flag <sup>1</sup>	85	+30	+30	+30
Speed	Vessel speed (cm/sec)	-	+32	+32	+32
NA	Unknown data contents	86	-	+35	+35
Depth	Sonar depth (cm)	87	+35	+40	+40
NA	Unknown data contents	-	-	-	+44-83
Sonar Beam	Sonar beam ID <sup>2</sup>	50	+40	+45	+85
Voltage	Voltage scale (1/10 volt)	51	+42	+47	+87
Frequency	Sonar beam frequency (Hz)	92	+44	+49	+89
NA	Unknown data contents	-	+48-60	+53-65	+89-145
Return Count	Number ping returns ( $n$ )	A0	+62	+67	+147
Header End	End of ping header	21	+66	+72	+152
Ping Returns	Sonar intensity [0-255]	21	+67	+73	+153
Ping #2	Beginning of ping #2	21	+67+ $n$ +1	+73+ $n$ +1	+152+ $n$ +1
... <sup>3</sup>	...	...	...	...	...

<sup>1</sup> 0=bad; 1=good.

<sup>2</sup> 0=Down Scan Low Freq.; 1=Down Scan Hi Freq.; 2=Side Scan Port-side; 3=Side Scan Starboard;  
4=Down Scan Megahertz.

<sup>3</sup> Pattern repeats for duration of sonar recording.

**Table 2.** Computation time for sequential and multi-threaded algorithms on a test dataset<sup>c</sup>.

Threads ( <i>t</i> )	Sequential Algorithms <sup>b</sup>	Decode SON <sup>c</sup>	Bedpick Plots <sup>c</sup>	Sonogram Tiles <sup>c</sup>	Rectify Sonograms <sup>c</sup>	Total (s)	Total (hh:mm:ss)
1	367.3	52.8	423.3	1158.6	4349.0	6351.0	01:45:51
2	363.4	35.3	261.0	723.2	3197.1	4580.0	01:16:20
4	361.5	25.7	186.7	531.2	1960.9	3066.0	00:51:06
6	359.0	23.9	179.6	533.7	1451.8	2548.0	00:42:28
8	363.2	24.0	175.8	522.1	1388.9	2474.0	00:41:14

<sup>a</sup> Test dataset from a Humminbird Helix with Mega imaging. Sonar recording includes high-frequency down image (200 kHz), very high-frequency down image (1.2 MHz), and two very high-frequency side scan images (1.2 MHz). Total duration of the recording is 01:00:06 (hh:mm:ss). Total ping count is 279,915. Range setting is 1,398 returns per ping, or 26.6m.

<sup>b</sup> Sequential (e.g., non-parallel) algorithms include decoding DAT file, determining SON file structure, depth processing, trackline smoothing, and generating rectified mosaics.

<sup>c</sup> Multi-threaded processing algorithm.

## References

358

- 359 Andreadis, K. M., Schumann, G. J. P., & Pavelsky, T. (2013). A simple global river  
360 bankfull width and depth database. *Water Resources Research*, *49*(10), 7164–  
361 7168. doi: <https://doi.org/10.1002/wrcr.20440>
- 362 Barnosky, A. D., Matzke, N., Tomiya, S., Wogan, G. O. U., Swartz, B., Quental,  
363 T. B., ... Ferrer, E. A. (2011). Has the Earth’s sixth mass extinction already  
364 arrived? *Nature*. doi: <https://doi.org/10.1038/nature09678>
- 365 Biggs, J., von Fumetti, S., & Kelly-Quinn, M. (2017). The importance of small  
366 waterbodies for biodiversity and ecosystem services: implications for policy  
367 makers. *Hydrobiologia*, *793*(1), 3–39. doi: [10.1007/s10750-016-3007-0](https://doi.org/10.1007/s10750-016-3007-0)
- 368 Blondel, P. (2009). *The Handbook of Sidescan Sonar*. Berlin, Heidelberg: Springer  
369 Berlin Heidelberg. doi: <https://doi.org/10.1007/978-3-540-49886-5>
- 370 Bock, M., Xofis, P., Mitchley, J., Rossner, G., & Wissen, M. (2005). Object-oriented  
371 methods for habitat mapping at multiple scales – Case studies from Northern  
372 Germany and Wye Downs, UK. *Journal for Nature Conservation*, *13*(2-3),  
373 75–89. doi: <https://doi.org/10.1016/j.jnc.2004.12.002>
- 374 Bodine, C. S., & Buscombe, D. (2022). *PING-Mapper [Computer Software]*. doi:  
375 <https://doi.org/10.5281/zenodo.6604785>
- 376 Brown, C. J., Smith, S. J., Lawton, P., & Anderson, J. T. (2011). Benthic habitat  
377 mapping: A review of progress towards improved understanding of the spatial  
378 ecology of the seafloor using acoustic techniques. *Estuarine, Coastal and Shelf  
379 Science*, *92*(3), 502–520. doi: <https://doi.org/10.1016/j.ecss.2011.02.007>
- 380 Buscombe, D. (2017). Shallow water benthic imaging and substrate characteri-  
381 zation using recreational-grade sidescan-sonar. *Environmental Modelling and  
382 Software*, *89*, 1–18. doi: <https://doi.org/10.1016/j.envsoft.2016.12.003>
- 383 Buscombe, D., & Goldstein, E. B. (2022). A Reproducible Pipeline for Geoscientific  
384 Image Segmentation with Fully Convolutional Models. *Earth and Space Sci-  
385 ence*.
- 386 Buscombe, D., Grams, P. E., & Smith, S. M. C. (2016). Automated Riverbed  
387 Sediment Classification Using Low-Cost Sidescan Sonar. *Journal of Hy-  
388 draulic Engineering*, *142*(2), 6015019. doi: [https://doi.org/10.1061/  
389 \(ASCE\)HY.1943-7900.0001079](https://doi.org/10.1061/(ASCE)HY.1943-7900.0001079)
- 390 Cael, B. B., Heathcote, A. J., & Seekell, D. A. (2017). The volume and mean depth  
391 of Earth’s lakes. *Geophysical Research Letters*, *44*(1), 209–218. doi: [https://  
392 doi.org/10.1002/2016GL071378](https://doi.org/10.1002/2016GL071378)
- 393 Cheek, B. D., Grabowski, T. B., Bean, P. T., Groeschel, J. R., & Magnelia, S. J.  
394 (2016). Evaluating habitat associations of a fish assemblage at multiple spa-  
395 tial scales in a minimally disturbed stream using low-cost remote sensing.  
396 *Aquatic Conservation: Marine and Freshwater Ecosystems*, *26*(1), 20–34. doi:  
397 [10.1002/aqc.2569](https://doi.org/10.1002/aqc.2569)
- 398 Chesterman, W. D., Clynick, P. R., & Stride, A. H. (1958). An acoustic aid to sea  
399 bed survey. *Acta Acustica united with Acustica*, *8*(5).
- 400 Cobra, D. T., Oppenheim, A. V., & Jaffe, J. S. (1992). Geometric Distor-  
401 tions in Side-Scan Sonar Images: A Procedure for Their Estimation and  
402 Correction. *IEEE Journal of Oceanic Engineering*, *17*(3), 252–268. doi:  
403 <https://doi.org/10.1109/48.153442>
- 404 Danovaro, R., Company, J. B., Corinaldesi, C., D’Onghia, G., Galil, B., Gambi, C.,  
405 ... Tselepides, A. (2010). Deep-Sea Biodiversity in the Mediterranean Sea:  
406 The Known, the Unknown, and the Unknowable. *PLOS ONE*, *5*(8), e11832.  
407 doi: <https://doi.org/10.1371/JOURNAL.PONE.0011832>
- 408 Dolloff, C. A., & Warren, M. L., Jr. (2003). Fish Relationships with Large Wood  
409 in Small Streams. In S. V. Gregory, K. L. Boyer, & A. M. Gurnell (Eds.), *The  
410 ecology and management of wood in world rivers* (Vol. 37, pp. 179–193). Amer-  
411 ican Fisheries Society. doi: <https://doi.org/10.47886/9781888569568.ch9>

- 412 Flowers, H. J., & Hightower, J. E. (2013). A Novel Approach to Surveying Stur-  
 413 geon Using Side-Scan Sonar and Occupancy Modeling. *Marine and Coastal*  
 414 *Fisheries*, 5(1), 211–223. doi: 10.1080/19425120.2013.816396
- 415 Fu, H., Zhong, J., Yuan, G., Ni, L., Xie, P., & Cao, T. (2014). Functional traits  
 416 composition predict macrophytes community productivity along a water depth  
 417 gradient in a freshwater lake. *Ecology and Evolution*, 4(9), 1516–1523. doi:  
 418 10.1002/ece3.1022
- 419 Gocłowski, M. R., Kaeser, A. J., & Sammons, S. M. (2013). Movement and Habi-  
 420 tat Differentiation among Adult Shoal Bass, Largemouth Bass, and Spotted  
 421 Bass in the Upper Flint River, Georgia. *North American Journal of Fisheries*  
 422 *Management*, 33(1), 56–70. doi: 10.1080/02755947.2012.741555
- 423 Gumusay, M. U., Bakirman, T., Tuney Kizilkaya, I., & Aykut, N. O. (2019). A  
 424 review of seagrass detection, mapping and monitoring applications using  
 425 acoustic systems. *European Journal of Remote Sensing*, 52(1), 1–29. doi:  
 426 10.1080/22797254.2018.1544838
- 427 Holcomb, K. M., Schueller, P., Jelks, H. L., Knight, J. R., & Allen, M. S. (2020).  
 428 Use of Strong Habitat–Abundance Relationships in Assessing Popula-  
 429 tion Status of Cryptic Fishes: An Example Using the Harlequin Darter.  
 430 *Transactions of the American Fisheries Society*, 149(3), 320–334. doi:  
 431 <https://doi.org/10.1002/tafs.10231>
- 432 Johansen, M. (2013). *HumViewer (Version 86) [Computer Software]*. Retrieved from  
 433 <https://humviewer.cm-johansen.dk/>
- 434 Kaeser, A. J., & Litts, T. L. (2008). An Assessment of Deadhead Logs and Large  
 435 Woody Debris Using Side Scan Sonar and Field Surveys in Streams of South-  
 436 west Georgia. *Fisheries*, 33(12), 589–597. doi: [https://doi.org/10.1577/](https://doi.org/10.1577/1548-8446-33.12.589)  
 437 [1548-8446-33.12.589](https://doi.org/10.1577/1548-8446-33.12.589)
- 438 Kaeser, A. J., & Litts, T. L. (2010). A Novel Technique for Mapping Habitat in  
 439 Navigable Streams Using Low-cost Side Scan Sonar. *Fisheries*, 35(4), 163–174.  
 440 doi: <https://doi.org/10.1577/1548-8446-35.4.163>
- 441 Kaeser, A. J., Litts, T. L., & Tracy, T. W. (2013). Using low-cost side-scan sonar  
 442 for benthic mapping throughout the lower Flint River, Georgia, USA. *River*  
 443 *Research and Applications*, 29(5), 634–644. doi: [https://doi.org/10.1002/](https://doi.org/10.1002/rra.2556)  
 444 [rra.2556](https://doi.org/10.1002/rra.2556)
- 445 Kaeser, A. J., Smit, R., & Gangloff, M. (2019). *Mapping and modeling the distri-*  
 446 *bution, abundance, and habitat associations of the endangered fat threeridge in*  
 447 *the Apalachicola river system* (Vol. 10) (No. 2). U.S. Fish and Wildlife Service.  
 448 doi: 10.3996/032019-JFWM-021
- 449 Kerr, J. T., & Ostrovsky, M. (2003). From space to species: ecological applica-  
 450 tions for remote sensing. *Trends in Ecology & Evolution*, 18(6), 299–305. doi:  
 451 [https://doi.org/10.1016/S0169-5347\(03\)00071-5](https://doi.org/10.1016/S0169-5347(03)00071-5)
- 452 Klein, M., & Edgerton, H. (1968). Sonar a modern technique for ocean exploita-  
 453 tion. *IEEE Spectrum*, 5(6), 40–46. doi: [https://doi.org/10.1109/MSPEC.1968](https://doi.org/10.1109/MSPEC.1968.5214684)  
 454 [.5214684](https://doi.org/10.1109/MSPEC.1968.5214684)
- 455 Leraand Engineering Inc. (2022). *SonarTRX [Computer Software]*. Retrieved from  
 456 <https://www.sonartrx.com/>
- 457 Longhurst, A. R. (2007). *Ecological Geography of the Sea* (Second ed.). Elsevier Inc.  
 458 doi: <https://doi.org/10.1016/B978-0-12-455521-1.X5000-1>
- 459 Murphy, K. J. (2021). Open-Source Science: The NASA Earth Science Perspective.  
 460 *The Earth Observer*. Retrieved from [https://earthdata.nasa.gov/learn/](https://earthdata.nasa.gov/learn/articles/open-source-science-nasa-earth-science-perspective)  
 461 [articles/open-source-science-nasa-earth-science-perspective](https://earthdata.nasa.gov/learn/articles/open-source-science-nasa-earth-science-perspective)
- 462 Musale, A. S., & Desai, D. V. (2010). Distribution and abundance of macroben-  
 463 thic polychaetes along the South Indian coast. *Environmental Monitoring and*  
 464 *Assessment* 2010 178:1, 178(1), 423–436. doi: [https://doi.org/10.1007/S10661](https://doi.org/10.1007/S10661-010-1701-3)  
 465 [-010-1701-3](https://doi.org/10.1007/S10661-010-1701-3)
- 466 Myrvold, K. M., & Dervo, B. K. (2020). Flight elevation and water clarity affect



- 467 the utility of unmanned aerial vehicles in mapping stream substratum. *Fish-*  
 468 *eries Management and Ecology*, 27(2), 167–169. doi: [https://doi.org/10.1111/](https://doi.org/10.1111/fme.12394)  
 469 [fme.12394](https://doi.org/10.1111/fme.12394)
- 470 Parnum, I. M., Ellement, T., Perry, M. A., Parsons, M. J., & Tecchiato, S. (2017).  
 471 Using recreational echo-sounders for marine science studies. In *Proceedings of*  
 472 *ACOUSTICS 2017*. Retrieved from [http://cmst.curtin.edu.au/products/](http://cmst.curtin.edu.au/products/humconverter-software/)  
 473 [humconverter-software/](http://cmst.curtin.edu.au/products/humconverter-software/)
- 474 Prechtel, A. R., Coulter, A. A., Etchison, L., Jackson, P. R., & Goforth, R. R.  
 475 (2018). Range estimates and habitat use of invasive Silver Carp (*Hypoph-*  
 476 *thalmichthys molitrix*): evidence of sedentary and mobile individuals. *Hydrobi-*  
 477 *ologia*, 805(1), 203–218. doi: 10.1007/s10750-017-3296-y
- 478 ReefMaster Software Ltd. (2021). *ReefMaster [Computer Software]*. Retrieved from  
 479 <https://reefmaster.com.au/>
- 480 Sánchez-Carnero, N., Rodríguez-Pérez, D., Couñago, E., Aceña, S., & Freire,  
 481 J. (2012). Using vertical Sidescan Sonar as a tool for seagrass cartogra-  
 482 phy. *Estuarine, Coastal and Shelf Science*, 115, 334–344. doi: 10.1016/  
 483 [j.ecss.2012.09.015](https://doi.org/10.1016/j.ecss.2012.09.015)
- 484 Schmidt, B. A., Tucker, T. R., Collier, J. J., Mayer, C. M., Roseman, E. F., Stott,  
 485 W., & Pritt, J. J. (2020). Determining habitat limitations of Maumee River  
 486 walleye production to western Lake Erie fish stocks: documenting a spawn-  
 487 ing ground barrier. *Journal of Great Lakes Research*, 46(6), 1661–1673. doi:  
 488 <https://doi.org/10.1016/j.jglr.2020.08.022>
- 489 Scholl, E. A., Cross, W. F., Baxter, C. V., & Guy, C. S. (2021). Uncovering pro-  
 490 cess domains in large rivers: Patterns and potential drivers of benthic sub-  
 491 strate heterogeneity in two North American riverscapes. *Geomorphology*, 375,  
 492 107524. doi: <https://doi.org/10.1016/j.geomorph.2020.107524>
- 493 Singh, H., Adams, J., Mindell, D., & Foley, B. (2000). Imaging underwater for ar-  
 494 chaeology. *International Journal of Phytoremediation*, 21(1), 319–328. doi:  
 495 <https://doi.org/10.1179/jfa.2000.27.3.319>
- 496 Smit, R., & Kaeser, A. J. (2016). Defining freshwater mussel mesohabitat associa-  
 497 tions in an alluvial, Coastal Plain river. *Freshwater Science*, 35(4), 1276–1290.  
 498 doi: 10.1086/688928
- 499 Smith, K. F., & Brown, J. H. (2002). Patterns of Diversity, Depth Range and  
 500 Body Size among Pelagic Fishes along a Gradient of Depth. *Global Ecol-*  
 501 *ogy and Biogeography*, 11(4), 313–322. doi: [https://doi.org/10.1046/](https://doi.org/10.1046/j.1466-822X.2002.00286.x)  
 502 [j.1466-822X.2002.00286.x](https://doi.org/10.1046/j.1466-822X.2002.00286.x)
- 503 Tickner, D., Opperman, J. J., Abell, R., Acreman, M., Arthington, A. H., Bunn,  
 504 S. E., . . . Young, L. (2020). Bending the Curve of Global Freshwater Biodi-  
 505 versity Loss: An Emergency Recovery Plan. *BioScience*, 70(4), 330–342. doi:  
 506 <https://doi.org/10.1093/BIOSCI/BIAA002>
- 507 Walker, D. J., & Alford, J. B. (2016). Mapping Lake Sturgeon Spawning Habitat  
 508 in the Upper Tennessee River using Side-Scan Sonar. *North American Jour-*  
 509 *nal of Fisheries Management*, 36(5), 1097–1105. doi: 10.1080/02755947.2016  
 510 .1198289
- 511 Weiers, S., Bock, M., Wissen, M., & Rossner, G. (2004). Mapping and indicator  
 512 approaches for the assessment of habitats at different scales using remote sens-  
 513 ing and GIS methods. *Landscape and Urban Planning*, 67(1-4), 43–65. doi:  
 514 [https://doi.org/10.1016/S0169-2046\(03\)00028-8](https://doi.org/10.1016/S0169-2046(03)00028-8)
- 515 Yan, J., Meng, J., & Zhao, J. (2021). Bottom detection from backscatter data of  
 516 conventional side scan sonars through 1d-unet. *Remote Sensing*, 13(5). doi:  
 517 <https://doi.org/10.3390/rs13051024>
- 518 Yang, J., Gong, P., Fu, R., Zhang, M., Chen, J., Liang, S., . . . Dickinson, R. (2013).  
 519 The role of satellite remote sensing in climate change studies. *Nature Climate*  
 520 *Change*, 3(10), 875–883. doi: <https://doi.org/10.1038/nclimate1908>
- 521 Zhao, W., Hu, A., Ni, Z., Wang, Q., Zhang, E., Yang, X., . . . Wang, J. (2019). Bio-

522           diversity patterns across taxonomic groups along a lake water-depth gradient:  
523           Effects of abiotic and biotic drivers. *Science of The Total Environment*, 686,  
524           1262–1271. doi: 10.1016/j.scitotenv.2019.05.381  
525       Zheng, G., Zhang, H., Li, Y., & Zhao, J. (2021). A Universal Automatic Bottom  
526       Tracking Method of Side Scan Sonar Data Based on Semantic Segmentation.  
527       *Remote Sensing*, 13(10), 1945. Retrieved from [https://www.mdpi.com/](https://www.mdpi.com/2072-4292/13/10/1945)  
528       2072-4292/13/10/1945 doi: <https://doi.org/10.3390/rs13101945>